The solution structure of DNA decamer duplex containing the Dewar product of thymidylyl(3′→5′)thymidine by NMR and full relaxation matrix refinement

Joon-Hwa Lee[a], Geum-Sook Hwang[a], Jong-Ki Kim[b], Byong-Seok Choi[a,*]

[a]*Department of Chemistry, Korea Advanced Institute of Science and Technology, 373-1, Kusong-dong, Yusong-gu, Taejon 305-701, South Korea*
[b]*Department of Biomedical Engineering, School of medicine, Catholic University of Taegu-Hyosung, Taegu 705-716, South Korea*

Received 6 February 1998; revised version received 6 April 1998

Abstract The (6-4) adducts and their Dewar isomers play an important role in cytotoxicity and mutation in skin cells exposed to sunlight. Structural study of the DNA duplex containing a site-specific photoproduct is an essential step toward understanding the molecular mechanism of the mutagenesis and the repair activity of UV-irradiated DNA. Here we use ^{1}H NMR spectroscopy and full relaxation matrix refinement to investigate the solution structure of the duplex Dewar decamer. We find that the isomerization of the (6-4) adduct to its Dewar form induces a substantial change in overall structure of the oligonucleotide duplex. Contrasting base stacking of two lesion sites results in a large difference in the structural impacts induced by the two photoproducts, such as differential disruption of hydrogen bonding at the lesion sites and overall helical bending of 44° by the (6-4) lesion and 21° by the Dewar lesion.

Key words: Dewar photoproduct; (6-4) Adduct; Photo-damaged DNA; Nuclear magnetic resonance spectroscopy; Solution structure; Full relaxation matrix refinement

1. Introduction

Sunlight-induced human skin cancer is thought to be due to mutations which result from DNA damage produced by the UV portion of the solar spectrum [1–5]. The major classes of cytotoxic, mutagenic, and carcinogenic DNA photoproducts induced by the UV portion of sunlight are *cis-syn* cyclobutane dimers and pyrimidine(6-4)pyrimidone adducts [1–7]. Pyrimidine(6-4)pyrimidone adducts involve a UV-induced covalent bond between the C6 and C4 of adjacent pyrimidines. The (6-4) adducts are not stable in sunlight but are converted to their Dewar valence isomers via absorption of UV-B irradiation (Fig. 1a) [8]. It has been reported that the Dewar isomers of the (6-4) adducts also play an important role in cytotoxicity and mutation in skin cells exposed to sunlight [5–7].

Structural study of the DNA duplex containing a site-specific photoproduct is an essential step toward understanding the molecular mechanism of the mutagenesis and the repair activity of UV-irradiated DNA. So far the solution structures of the (6-4) and Dewar products of the TpT dimer itself have been extensively studied by NMR spectroscopy [9–12]. Recently, three-dimensional solution structures of the DNA duplex decamers containing the (6-4) adduct and the *cis-syn* dimer were determined by NMR spectroscopy and the relaxation matrix refinement method [13,14]. However, the three-dimensional structures of the DNA duplex containing the Dewar product are not yet available. Herein, we report the first detailed three-dimensional solution structure of the DNA duplex decamer containing the Dewar product, d(CGCAT-[Dewar]TACGC)·d(GCGTAATGCG), which was determined by two-dimensional NMR spectroscopy and full relaxation matrix refinement. In addition, we present the differential structural changes of the DNA duplex decamers induced by the (6-4) adduct and Dewar product of TpT site.

*Corresponding author. Fax: (82) (42) 869-2810.
E-mail: bschoi@cais.kaist.ac.kr

Abbreviations: (6-4) adduct, pyrimidine(6-4)pyrimidone adduct; Dewar product, Dewar valence isomer of (6-4) adduct; NMR, nuclear magnetic resonance; UV-B, band B of ultraviolet irradiation with a wavelength of 280–320 nm; T[Dewar]T, Dewar product of a TpT site; HPLC, high pressure liquid chromatography; NOE, nuclear Overhauser effect; NOESY, nuclear Overhauser effect spectroscopy; duplex (6-4) decamer, (6-4)-adduct-containing duplex decamer; duplex Dewar decamer, Dewar-adduct-containing duplex decamer; PM-3, the third parameter method

2. Materials and methods

2.1. Sample preparation

The single-stranded oligonucleotides d(CGCATTACGC) and d(GCGTAATGCG) were synthesized by the phosphoramidite method on a DNA synthesizer (Applied Biosystem, model 391). The crude 5′-dimethoxy-tritiated oligonucleotides were deprotected by treatment with concentrated ammonia for 15–18 h at 55°C. The DNA products were purified by reverse-phase HPLC and desalted on a Sephadex G-25 column.

The thymine (6-4) adduct was produced by irradiating the oligonucleotide d(CGCATTACGC) in aqueous solution contained in a large Petri dish using a radiation reactor (New Southern England Ultraviolet Products, model RPR-2000) equipped with twelve 35-W germicidal lamps (254 nm) for 10–16 h. The average irradiating intensity was 80 J/m^2 s. The temperature of the reactor chamber was maintained around 10°C by purging with liquid nitrogen gas during irradiation. Irradiated samples were dried and fractionated using a preparative Hypersil C-18 HPLC column with a 60-min 8–16% methanol gradient in 20 mM sodium phosphate buffer, pH 7.0, at a flow rate of 2 ml/min. The (6-4) adduct, which was characterized by a maximum absorption band near 325 nm, was repurified by HPLC with a 60-min 7–12% methanol gradient in the above-mentioned buffer system and a Sephadex G-25 column.

The single-stranded decamer containing the (6-4) adduct was dissolved in 0.5 ml 99.996% D_2O and transferred to a 5-ml NMR tube. The sample was irradiated using the radiation reactor described above with a 313-nm sun-lamp filtered by Pyrex. The photoconversion to the Dewar product was monitored by ^{1}H NMR. The (6-4) adduct was quantitatively converted to its Dewar product in 1 h. The duplex Dewar decamer was prepared by dissolving the modified strand and the complementary strand adjusted to a stoichiometric 1:1 ratio in aqueous solutions.

2.2. NMR experiment

All NMR experiments were carried out using Bruker AMX-500 or

PII S0014-5793(98)00508-0

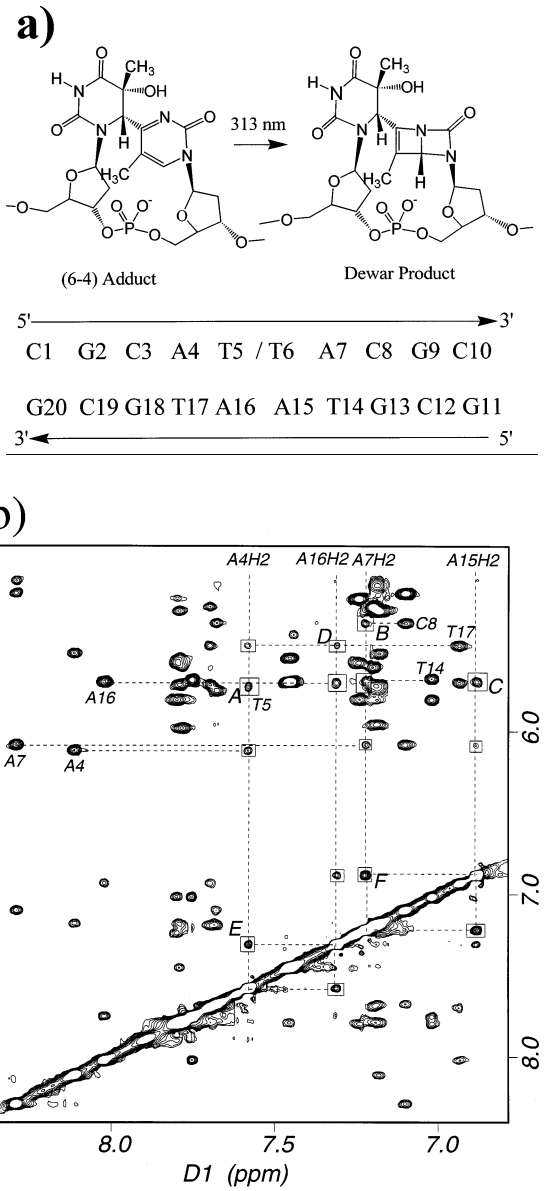

Fig. 1. a: DNA sequence context and chemical structures of the (6-4) adduct and its Dewar valence isomer. b: Expanded NOESY (250 ms mixing time) contour plot of the duplex Dewar decamer in 200 mM NaCl, pH 7.0, D_2O solution at 7°C. The figure shows NOE interactions of adenine H2 protons with H1′ protons of their 3′-side and own residue, and two interstrand NOEs between adenine H2 protons and neighboring adenine H2 protons, which are often associated with bending geometries of these duplexes. The labeled crosspeaks A–F in the figures are assigned as follows: A, A4(H2)↔T5(H1′); B, A7(H2)↔C8(H1′); C, A15(H2)↔A16(H1′); D, A16(H2)↔T17(H1′); E, A4(H2)↔A16(H1′); F, A7(H2)↔A15(H1′). c: Expanded NOESY (200 ms mixing time) contour plot of the duplex Dewar decamer in 200 mM NaCl, pH 7.0, H_2O solution at 1°C. Absence of NOE crosspeak between A16-H2 and T5-imino proton resonances indicates the disruption of Watson-Crick base pairing in the T5·A16 base pair. The labeled crosspeaks A–M in the figure are assigned as follows: A, T14(NH)↔A7(H2); B, T17(NH)↔A4(H2); C,E, G2(NH)↔C8(NH_2); D, G9(NH)↔C8(NH_2); F,G, G9(NH)↔C12(NH_2); H,J, G13(NH)↔A7(H2); I, G13(NH)↔A7(H2); K, G13(NH)↔C12(NH_2); L,N, G18(NH)↔C3(NH_2); M, G18(NH)↔A4(H2).

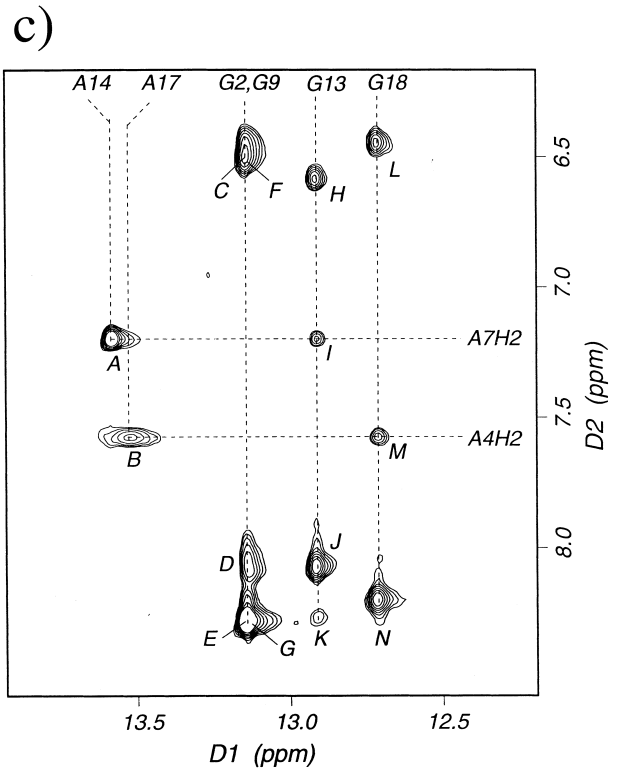

Fig. 1 (*continued*).

a DMX-600 spectrometers. The data were processed using a Silicon Graphics workstation with the program FELIX 95.0. The phase-sensitive NOESY spectra in D_2O solution were recorded with mixing times of 100 and 250 ms using time-proportional phase incrementation. The NOESY spectrum in H_2O solution at 1°C was recorded using a jump-and-return-pulse sequence for the reading pulse with mixing times of 200 ms. The spectra were acquired with 2000 data points in the t_2 dimension and 512 points in the t_1 dimension. The time-domain data were zero-filled in both directions to 2000×2000 and multiplied with a π/4- or π/3-shifted squared-sine function before Fourier transformation.

2.3. Structure determination

Initial structures of B-form DNA were generated and the T5–T6 sequence was modified to the Dewar form using the molecular modeling program INSIGHT II (INSIGHT II is the registered trademark of Biosym Technologies Inc., San Diego, CA 92121-27777, USA). The ideal geometry of the Dewar product of the TpT dimer was obtained from the structure calculated by the Semi Empirical PM3 method in the program HYPERCHEM. The 418 NMR-derived distance constraints in the duplex Dewar decamer were included in the distance-restrained molecular dynamics calculations. Simulations were carried out with a distance-dependent dielectric constant scheme using X-PLOR [15] installed on a Cray 270 supercomputer. During the equilibration period, which was performed at 500 K for 5 ps, the force constants for distance restraints were scaled up gradually to 147 kcal/mol. Productive dynamics were then simulated for 20 ps at 300 K. The trajectories of the last 6 ps were averaged, and averaged coordinates were subjected to restrained energy minimization by a Powell scheme. In order to account for potential spin diffusion effects, distance-refined structures were recalculated against NOE volume intensity data, which were measured at two mixing times of 100 and 250 ms. The methyl-group protons were $<r^{-3}>$ weighting averaged. During the equilibration at 400 K for 1 ps, the weighting factors for the intensity errors were scaled up gradually to 100 kcal/mol. Productive dynamics were then simulated for 10 ps at 300 K and the trajectories of the last 1 ps were averaged. The averaged coordinates were further subjected to Powell energy minimization. The helical parameters of the duplex decamer were determined by the program CURVES.

Table 1
The structure refinement statistics and analysis of duplex Dewar decamer

	Distance refinement[a]	Relaxation refinement[b]
Number of restraints		
Distance restraints (NOE)	418	236
Intensity restraints[c]	–	191
X-PLOR energies (kcal/mol)		
Total	−402.9 ± 35.4	−628.6 ± 27.7
NOE	177.4 ± 14.5	17.1 ± 1.1
Bond	98.3 ± 4.7	50.3 ± 1.2
Angle	388.8 ± 21.6	214.5 ± 6.7
Improper angle	7.8 ± 1.8	0.5 ± 0.1
VDW	−33.6 ± 13.2	−178.0 ± 0.9
Hydrogen bond	−148.6 ± 8.4	−138.2 ± 2.4
Relaxation	–	267.3 ± 26.8
Rms deviations		
From distance restraints	0.065 ± 0.002	0.027 ± 0.001
From idealized geometry		
: Bond lengths	0.022 ± 0.001	0.015 ± 0.001
: Bond angles	4.730 ± 0.149	3.401 ± 0.085
: Improper angles	1.252 ± 0.171	0.967 ± 0.059
$R^{1/6}$ value[d]	–	0.034 ± 0.001

[a]This column gives the average and standard deviations for indicated variables obtained from eight accepted structures of restrained molecular dynamics (distance refinement).
[b]This column gives the average and standard deviations for indicated variables obtained from five accepted structures for full relaxation matrix refinement.
[c]Intensity restraints were constructed by two sets of 191 intensity data which were measured at 100 and 250 ms mixing times.
[d]R value is used for assessing the quality of the final structure as a measure of the fit of the refined coordinates to the NOESY data. $R^{1/6} = \Sigma_{spectra}\Sigma_i^N\omega_i well(I_i^c, k_S I_i^o, \Delta_i, 1/6)/\Sigma_{spectra}\Sigma_i^N\omega_i(k_S I_i^o)^{1/6}$, where I_i^c and I_i^o are respectively the calculated and observed NOE intensities, ω_i is weight factor, k_S is calibration factor, well(a,b,Δ,1/6) is defined as the absolute value of the difference between 1/6th powers of a and b.

3. Results and discussion

The solution structure of the duplex (6-4) decamer was solved by two-dimensional NMR spectroscopy and full relaxation matrix refinement and has been reported in our previous paper [14]. The distance-restrained molecular dynamics for the duplex Dewar decamer were performed with 418 NMR-derived distance constraints. The computations yielded eight accepted structures which have an atomic root-mean-squared (rms) difference of 1.48 Å for all heavy atoms. Their average structure was refined against NOE volume intensities which were measured at 100 and 250 ms mixing times. The five refined structures with an atomic rms difference of 1.22 Å for all heavy atoms were obtained with low particular energy values, as well as no restraints violations and good covalent geometry. The $R^{1/6}$ value for NOE volume intensities was 0.034 for the duplex Dewar decamer. Statistical estimations are shown in Table 1.

The main conformational perturbation caused by the (6-4) adduct and Dewar product concerns their effects on global DNA curvature. Both duplex decamers are significantly bent at the lesion sites (Fig. 2a,b). These helical bends are consistent with the observation of NOEs between H2 protons of all adenine bases and H1′ protons of their 3′-side residues in

Table 2
Conformational comparison[a] of the duplex (6-4) and Dewar decamers

	Duplex (6-4) decamer				Duplex Dewar decamer			
Overall bending	44°				21°			
Backbone parameter	T5	A16	T6	A15	T5	A16	T6	A15
sugar puckering	*C3′-endo*	*C1′-exo*	*C2′-exo*	*O1′-endo*	*C2′-endo*	*C2′-endo*	*C3′-endo*	*C1′-exo*
χ (glycosyl bond) (°)	−149	−86	−61	−115	−52	−100	−37	−118
γ (°)	178	46	56	53	41	56	61	−165
δ (°)	89	126	105	85	143	142	87	107
ε (°)	−114	173	−169	−150	−115	−138	−12	−153
ζ (°)	−71	−96	−82	−154	−111	−79	113	−163
α (°)	−119	−70	149	32	−163	−78	−76	−48
β (°)	−150	167	−146	87	147	161	133	139
Base-base parameter	A4·T17		A7·T14		A4·T17		A7·T14	
Buckle (°)	2		−1		10		−7	
Propeller twist (°)	2		5		−5		36	
Opening (°)	−6		−3		−14		−1	
Inter-base pair parameter[b]	C3/A4	A4/T5	T6/A7	A7/C8	C3/A4	A4/T5[b]	T6/A7	A7/C8
Tilt (°)	1	−5	−2	0	−1	33	−7	7
Roll (°)	15	−15	−8	−33	−40	−3	−19	0
Twist (°)	25	26	45	43	35	70	−6	40

[a]All backbone and helical parameters were calculated with the program CURVES.
[b]The inter-base pair parameters at the base pair steps A4/T5 and T6/A7 of both duplexes were replaced by the inter-base parameters on the complementary strand.

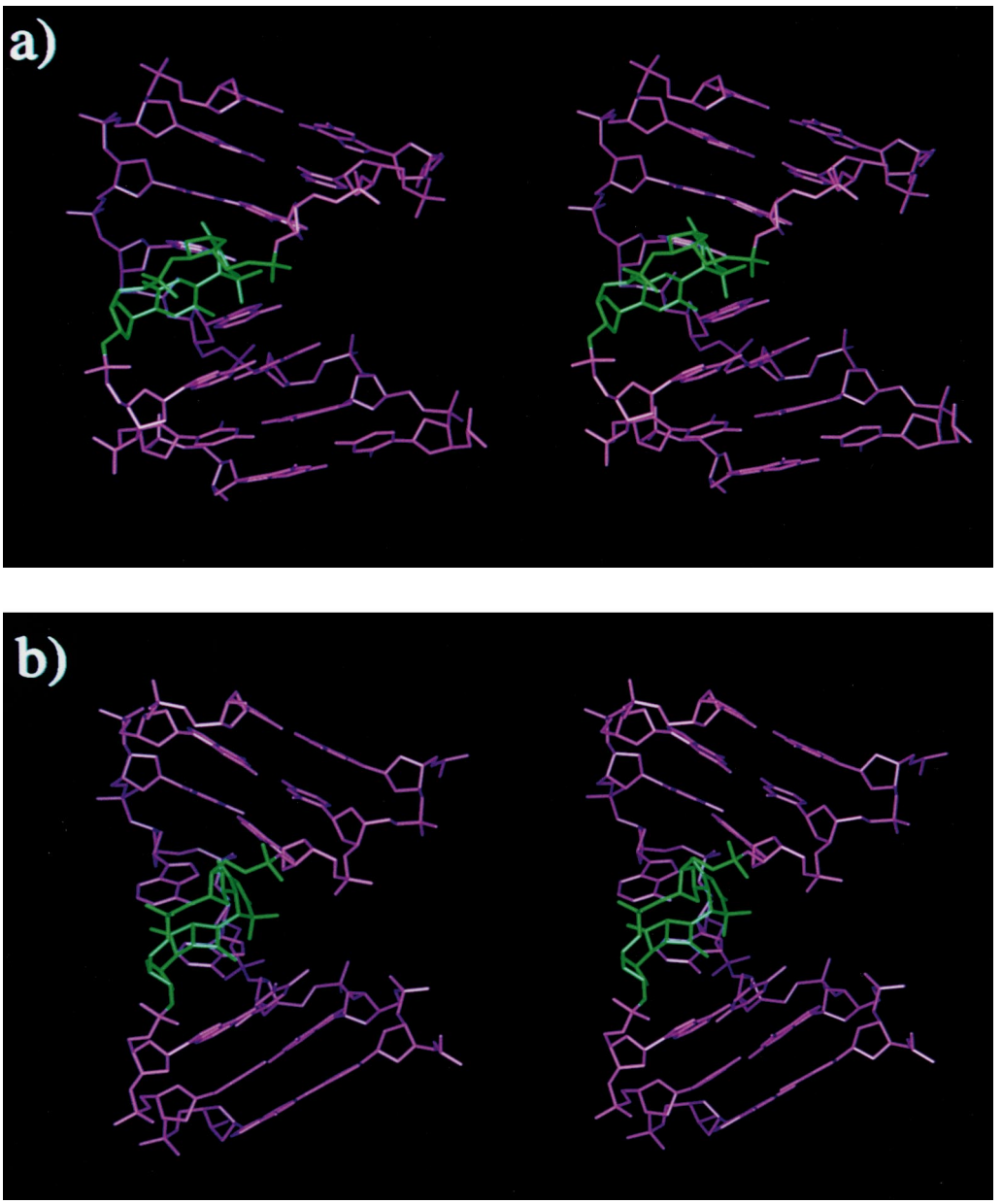

Fig. 2. Stereo pictures of the overall helix of (a) the duplex (6-4) and (b) Dewar decamers obtained by full relaxation matrix refinement. Overall helical bending of this duplex is 21°. The residues with green colored atoms are two thymine residues (T5, T6) of the (6-4) and Dewar lesions. The other residues are colored violet. The terminal base pairs and hydrogen atoms are excluded. All figures were obtained using the program INSIGHT II.

both duplexes, which are often associated with narrow minor grooves in the bending geometry (Fig. 1b) [14,16]. Overall helical bending induced by the (6-4) adduct and the Dewar product is 44° and 21°, respectively. Our previous structural studies [13] on the *cis-syn*-dimer-containing DNA duplex concluded that the dimer caused the DNA to bend by 9°. It was reported that the *cis-syn*, (6-4), and Dewar photoproducts were recognized by *Escherichia coli* damage recognition protein (UvrA) with a relative affinity of 1:9:4 [17,18]. When considering that the bending geometry at the DNA lesion site is the structural element that is best recognized by the repair enzyme [19], our data suggest that the large structural distortion induced by the (6-4) lesion may ensure a favorable recognition by the repair enzyme, which may explain the correlation with the higher repair rate of the T-T (6-4) adduct than of the T-T Dewar product and the T-T *cis-syn* dimer.

Probably the most interesting structural perturbation concerns base pairing at the thymine residues of the lesion sites. The structure of the (6-4) adduct inside the duplex shows a distinctive base orientation due to (6-4) covalent linkage which makes a normal Watson-Crick-type hydrogen bonding unfavorable at the 3′-side of the lesion site with an empty space between the 3′-thymine (T6) and its opposite base (A15) (Fig. 3a). This position is known to be substituted with a guanine residue rather than adenine during replication, leading to a predominantly 3′-T→C transition with 85% replicating error rate [20]. Smith et al. proposed a model to explain the high mutability and specificity of the (6-4) adduct at

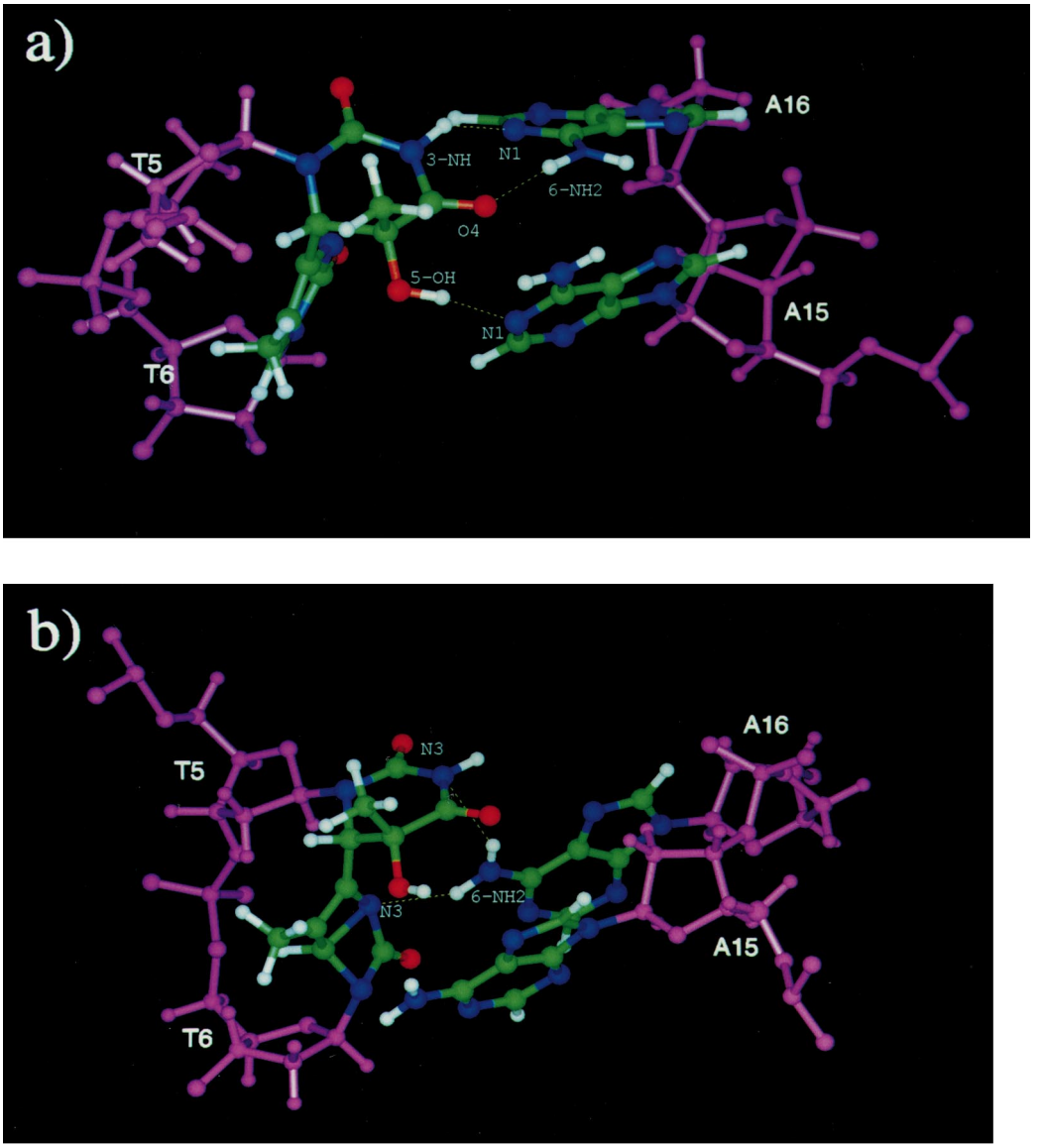

Fig. 3. Two base pairs (T5·A16 and T6·A15) in lesion sites of (a) the duplex (6-4) and (b) Dewar decamers. The base atoms in these figures are colored as atomic color representation: white, hydrogen; green, carbon; blue, nitrogen; red, oxygen. The atoms in the sugar backbone are colored violet. The dot lines colored yellow indicate available hydrogen bonds calculated by the program INSIGHT II. The standard Watson-Crick base pair of the T5 residue is retained in the (6-4) adduct, but the amino proton of the A16 residue makes a hydrogen bond with the lone pair of N3 nitrogen atoms of the T5 and T6 residues in the Dewar product. These figures were obtained using the program INSIGHT II.

the T-T site which may arise from the formation of a pyrimidone·guanine base pair via hydrogen bonds at O2 carbonyl in the pyrimidone ring [21]. However, our refined structure shows that such hydrogen bonding in a corresponding base pair is improbable under this geometry.

The hydrogen bonding features of the thymine residues at Dewar lesion site are much different from those of the (6-4) adduct. First of all, contrary to the duplex (6-4) decamer which retains a hydrogen-bonded imino proton at the 5′-side (T5) of the (6-4) lesion, the T5 imino proton of the Dewar lesion is not hydrogen-bonded (Fig. 3b). These results are consistent with the absence of an observed NOE crosspeaks between A16-H2 and T5-imino proton resonances in the duplex Dewar decamer (Fig. 1c), which NOE crosspeak was significantly observed in the duplex (6-4) decamer [14]. Secondly, when the (6-4) adduct is isomerized to the Dewar product, the lone pair on the O2 carbonyl of 3′-pyrimidone ring (T6) becomes more oriented away from the opposite strand, while the lone pair on N3 becomes geometrically oriented toward the opposite strand and, strikingly, can make hydrogen bonding to the amino proton of the A15 rather than the A16 residue in the opposite strand. This abnormal hydrogen bonding severely perturbs the base stacking between the A4·T17 and T5·A16 base pairs, which maintains the usual base stacking in the duplex (6-4) decamer. It is noted that the major conformational changes upon isomerization are observed at the 5′-side of the lesion in the form of a disruption of hydrogen bonding and a perturbation of the stacking interaction of the T5 residue, although the structural change caused by photoconversion of a (6-4) adduct to the Dewar isomer occurs in the pyrimidone ring of the T6 residue.

The major distortions in DNA backbone conformations of the lesion site or in the vicinity of the lesion are evident from Table 2. The (6-4) adduct and Dewar product show significant

differential effects on DNA backbone conformation. The glycosyl bond torsion angle χ at the T5 residue of the (6-4) lesion remains in the *anti* conformation, while the *high-anti* conformation predominates on the T5 residue of the Dewar lesion. This observation is consistent with the lack of a NOE for A4-H1′ ↔ T5-H6 residing on the 5′-side of the Dewar lesion [16]. The deoxyribose ring conformations and helical parameters at the 5′-side of the lesions also contrast with each other. *C3′-endo* sugar puckering has been observed in the T5 residue of the (6-4) lesion, while the *C2′-endo* conformation occurs on the T5 residue of the Dewar lesion. The twist angle at the C3/A4 base pair step of the Dewar lesion is 35° but the same step of the (6-4) lesion is twisted by 25°. The disruption of base stacking between the A4·T17 and T5·A16 base pairs of the Dewar lesion is parallel with the observation of much higher tilt and twist angles in this base step than in the (6-4) adduct.

The structural basis of absent hydrogen bonding at both thymine residues of the Dewar lesion may suggest a significant correlation with the observation that the (6-4) adduct is highly specific for the mutation induced under SOS condition in *E. coli* while the Dewar isomer induces a broad range of mutations. The lack of hydrogen bonding in the Dewar lesion site probably allows accommodation of mutations with less overall distortion compared with the (6-4) adduct.

Acknowledgements: This work was supported by the Korea Science and Engineering Foundation through the Center for Molecular Catalysis at Seoul National University, Korea Science and Engineering Foundation (Grant 981-0304-02-2), and the academic research fund of the Ministry of Education, Republic of Korea.

References

[1] Cleaver, J.E., Cortés, F., Karentz, D., Lutze, L.H., Morgan, W.F., Player, A.N., Vuksanovic, L. and Mitchell, D.L. (1988) Photochem. Photobiol. 48, 41–49.
[2] Mitchell, D.L. (1988) Photochem. Photobiol. 48, 51–57.
[3] Brash, D.E. (1988) Photochem. Photobiol. 48, 59–66.
[4] Mitchell, D.L. and Nairn, R.S. (1989) Photochem. Photobiol. 49, 805–819.
[5] Smith, C.A. and Taylor, J.-S. (1993) J. Biol. Chem. 268, 11143–11151.
[6] Zhao, X. and Taylor, J.-S. (1994) J. Am. Chem. Soc. 116, 8870–8876.
[7] Pfeifer, G.P. (1997) Photochem. Photobiol. 65, 270–283.
[8] Taylor, J.-S., Lu, H.-F. and Kotyk, J.J. (1990) Photochem. Photobiol. 51, 161–167.
[9] Kan, L.-S., Voituriez, L. and Cadet, J. (1988) Biochemistry 27, 5796–5803.
[10] Douki, T. and Cadet, J. (1994) Biochemistry 33, 11942–11950.
[11] Taylor, J.-S., Garrett, D.S. and Cohrs, M.P. (1988) Biochemistry 27, 7206–7215.
[12] Kan, L.-S., Voituriez, L. and Cadet, J. (1992) J. Photochem. Photobiol. B Biol. 12, 339–357.
[13] Kim, J.-K., Patel, D.J. and Choi, B.-S. (1995) Photochem. Photobiol. 62, 44–50.
[14] Kim, J.-K. and Choi, B.-S. (1995) Eur. J. Biochem. 228, 849–854.
[15] Brünger, A.T. (1992) X-PLOR Version 3.1, Yale University Press, New Haven, CT.
[16] Hwang, G.-S., Kim, J.-K. and Choi, B.-S. (1996) Eur. J. Biochem. 235, 359–365.
[17] Reardon, J.T., Nichols, A.F., Keeney, S., Smith, C.A., Taylor, J.-S., Linn, S. and Sancar, A. (1993) J. Biol. Chem. 268, 21301–21308.
[18] Svoboda, D.L., Smith, C.A., Taylor, J.-S. and Sancar, A. (1993) J. Biol. Chem. 268, 10694–10700.
[19] Vassylyev, D.G., Kashiwagi, T., Mikami, Y., Ariyoshi, M., Iwai, S., Ohtsuka, E. and Morikawa, K. (1995) Cell 83, 773–782.
[20] LeClerc, J.E., Borden, A. and Lawrence, C.W. (1991) Proc. Natl. Acad. Sci. USA 88, 9685–9689.
[21] Smith, C.A., Wang, M., Jiang, N., Che, L., Zhao, X. and Taylor, J.-S. (1996) Biochemistry 35, 4146–4154.